Boltzmann dynamics and temperature dependence of energy loss: Towards an understanding of the R_{AA} and v_2 puzzle for D-Mesons

To cite this article: F Scardina *et al* 2015 *J. Phys.: Conf. Ser.* **636** 012017

Journal of Physics: Conference Series **636** (2015) 012017 doi:10.1088/1742-6596/636/1/012017

Boltzmann dynamics and temperature dependence of energy loss: Towards an understanding of the R_{AA} and v_2 puzzle for D-Mesons

F. Scardina [1,2], S. K. Das[1,2], S. Plumari[1,2] and V. Greco[1,2]

[1] Department of Physics and Astronomy, University of Catania, Via S. Sofia 64, I- 95125 Catania, Italy

[2] Laboratori Nazionali del Sud, INFN-LNS, Via S. Sofia 62, I-95123 Catania, Italy

E-mail: scardinaf@lns.infn.it

Abstract. The two key observables related to heavy quarks that have been measured in experiments are the nuclear suppression factor R_{AA} and the elliptic flow v_2. Reproducing these two observables simultaneously is a puzzle which have challenged all the existing models. We have studied two ingredients responsible to address a large part of such a puzzle: the temperature dependence of the energy loss and the full solution of the Boltzmann collision integral for the scattering between the heavy quarks and the particle of the bulk. We have considered four different models to evaluate the temperature dependence of drag and diffusion coefficients of the heavy quark. All these four different models are set to reproduce the same $R_{AA}(p_T)$ measured in experiments at RHIC and LHC energy. We have found that for the same $R_{AA}(p_T)$ one can generate 2-3 times more v_2 depending on the temperature dependence of the heavy quarks drag coefficient. Moreover comparing the Fokker-Planck and the Boltzmann approach we have found that the latter seems more efficient into reproducing the elliptic flow for the same R_{AA}. Even a larger difference between the two approaches emerges from the comparison of a more differential observable, the $c\bar{c}$ angular correlation.

1. Introduction

The ultra-Relativistic Heavy Ion Collisions (uRHIC) performed at the Relativistic Heavy Ion Collider (RHIC) and at the Large Hadron Collider (LHC) have given clear indications that a Quark Gluon Plasma has been created in laboratory. Beyond the light quark and gluons, which constitute the bulk, Heavy Quarks (HQ), charm and bottom, are created in the collisions. The interest in the study of HQ as probes to characterize the QGP [1, 2] is due to the fact that they are created essentially in the early stage of the collisions and since their masses are much larger than the temperature of the medium, they are decoupled from the bulk during the entire dynamical evolution of the system. Moreover their masses are larger than the typical momentum exchanged during the collisions with the light quark and gluons and thus they undergone to a Brownian motion which can be described by means of the Fokker-Planck equations. In such an approach the interaction is encoded in the drag and in the diffusion coefficients. The two key observables related to HQ that have been measured in experiments are the nuclear suppression factor R_{AA} and the elliptic flow v_2. However lately also a more differential observable, the $c\bar{c}$ angular correlation, has been proposed to characterize the QGP.

Several theoretical efforts have been made to reproduce the R_{AA} and the v_2 observed in experiments [3, 4, 5, 6, 7] within the Fokker Planck (FP) approach [8, 9, 10, 11, 12, 13, 14, 15, 16, 17, 18, 19, 20, 21] and the relativistic Boltzmann approach (BM)[22, 23, 24, 25, 26, 27, 28, 29]. However all the approaches show some difficulties to describe simultaneously R_{AA} and v_2. We have found that two ingredients assume a particular importance in reducing the differences between experimental data for R_{AA} and v_2 and theoretical calculations: the temperature dependence of the interaction and the use of full Boltzmann collision integral to study the time evolution of HQ momentum .

The proceeding is organized as follows. In section 2 we discuss the Fokker Planck approach which is used to describe the propagation of heavy quark through the QGP. In this section four different modelings to calculate the drag and diffusion coefficients, entailing different temperature dependence of the drag coefficients, will be presented. In section 4 and 5 we compare the FP approach and the BM approach analyzing three observables: R_{AA}, v_2 and $c\bar{c}$ angular correlation and finally section 6 contains the conclusions.

2. Fokker-Planck approach

The propagation of the Heavy quark is described by the Fokker Planck equations indicated here

$$\frac{\partial f}{\partial t} = \frac{\partial}{\partial p_i}\left[A_i(\mathbf{p})f + \frac{\partial}{\partial p_j}[B_{ij}(\mathbf{p})]\right] \tag{1}$$

where A_i and B_{ij} are the drag and the diffusion coefficients. To study the propagation of HQ this equation is replaced by an equivalent equation, the relativistic Langevin equation, which is more suited for numerical simulations

$$\begin{aligned} dx_i &= \frac{p_i}{E}dt, \\ dp_i &= -Ap_i dt + (\sqrt{2B_0}P_{ij}^{\perp} + \sqrt{2B_1}P_{ij}^{\parallel})\rho_j\sqrt{dt} \end{aligned} \tag{2}$$

where dx_i and dp_i are the coordinates and momenta changes in each time step dt; A is the drag force and B_0 and B_1 are respectively the longitudinal and the transverse diffusion coefficients; ρ_j is the stochastic Gaussian distributed variable; $P_{ij}^{\perp} = \delta_{ij} - p_i p_j/p^2$ and $P_{ij}^{\parallel} = p_i p_j/p^2$ are the transverse and longitudinal projector operators respectively. We employ the common assumption, $B_0 = B_1 = D$ [9, 10, 11, 13, 15, 16].

To solve the Langevin equation a background medium which describes the evolution of the bulk is necessary. Usually Hydrodynamical simulation are employed to describe the expansion and cooling down of the bulk. In this work instead the evolution of the bulk is provided by a 3+1D relativistic transport code tuned at fixed η/s [30, 31] which is able to reproduce the same results of hydrodynamical simulations. The transport code provides at each time step the density profile and the temperature profile of the bulk. The knowledge of the local density and of the local temperature at each time step are necessary to calculate the drag coefficients.

To generate the bulk profile we have performed simulations of $Au+Au$ collisions at $\sqrt{s} = 200$ AGeV for the minimum bias and $Pb+Pb$ at $\sqrt{s} = 2.76$ ATeV energy for centralities $0-20\%$ and $30-50\%$. In both cases the initial conditions in coordinate space are given by the Glauber model, while in the momentum space a Boltzmann-Juttner distribution function up to a transverse momentum $p_T = 2$ GeV has been considered. At larger momenta mini-jet distributions, as calculated within pQCD at NLO order, have been employed [32]. At RHIC energy, $Au + Au$ at $\sqrt{s} = 200$, the maximum initial temperature of the fireball at the center is $T_i = 340$ MeV and the initial time for the fireball simulations is $\tau_i = 0.6$ fm/c. At LHC instead the initial maximum temperature at the center of the fireball is $T_0 = 510$ MeV and the initial time for the simulations is $\tau_0 \sim 1/T_0 = 0.3$ fm/c.

HQ are initially distributed in coordinate space according to the number of binary collisions extracted from the Glauber model. The HQ distribution in momentum space is in accordance with the one in proton-proton that have been taken from [33]. In this present work four different modelings are used to calculate the drag coefficient, entailing different temperature dependence. The diffusion coefficient is instead calculated in accordance with the Einstein relation $D = \Gamma ET$. Our purpose is to investigate how for fixed R_{AA} the v_2 develops under different temperature dependence of the energy loss.

Model-I (pQCD) - We have considered elastic interaction among HQ and the bulk (light quarks and gluons). The scattering matrix related to these process $\mathcal{M}_{gHQ}$, $\mathcal{M}_{qHQ}$ and $\mathcal{M}_{\bar{q}HQ}$ in leading order are the well known Combridge matrix that includes s, t, u channel and their interferences terms [34]. The t-channel develops the well know infrared singularity that is regularized introducing a Debye screening mass $m_D = \sqrt{4\pi\alpha_s}\,T$ with a running coupling [35].
Model-II (AdS/CFT) - A drag force from the gauge/string duality [36] have been also considered in which the drag coefficient can be evaluated through the following equation

$$\Gamma_{conf} = C\frac{T^2_{QCD}}{M_c} \tag{3}$$

where $C = \frac{\pi\sqrt{\lambda}}{2\sqrt{3}} = 2.1 \pm 0.5$. Studies of dynamical evolution of heavy quarks within the Langevin dynamics using AdS/CFT can be found in Ref. [12, 19].
Model-III (QPM) - We have also evaluated the drag coefficient considering a bulk consisting of particles with a T-dependent quasi-particle masses, $m_q = 1/3g^2T^2$, $m_g = 3/4g^2T^2$. This model is able to successfully reproduce the thermodynamics of lQCD [37] (see also [38, 39]) by fitting the coupling $g(T)$. Such a fit leads to the following coupling [37]:

$$g^2(T) = \frac{48\pi^2}{[(11N_c - 2N_f)ln[\lambda(\frac{T}{T_c} - \frac{T_s}{T_c})]^2} \tag{4}$$

where λ=2.6 and T/T_s=0.57.
Model-IV ($\alpha_{QPM}(T), m_q = m_g = 0$) - We have also considered a case where the light quarks and gluons are massless but the coupling is from the QPM as indicated in Eq. 4. This last case has to be considered as an expedient to have a drag which decreases with the temperature.

For all the four cases considered the interaction has been rescaled to reproduce the R_{AA}

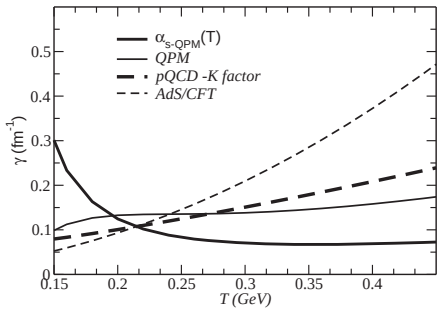

Figure 1. Variation of the drag coefficients with respect to temperature at $p = 5GeV$

observed in experiments. These rescaled drag coefficients have been shown in figure 1 as a function of temperature for the four different models. We observe that for all the modellings, with the exception of the *Model-IV ($\alpha_{QPM}(T), m_q = m_g = 0$)*, the drag is an increasing function of the temperature. The dependence of the drag on T is proportional to T^2 for the AdS/CFT

while it is much milder for the QPM. The increasing of the drag with T in the *Model-IV* ($\alpha_{QPM}(T), m_q = m_g = 0$) is instead due to the increasing of the coupling at low temperatures. An increasing drag coefficient with the temperature implies that the interaction between the heavy quarks and the bulk is stronger in the latter stages of the fireball evolution.
Having the density and temperature profile of the bulk, provided by the Boltzmann code, we have simulated the Langevin dynamics for the four different models presented above. The Langevin equation gives as output the momentum distributions of HQ at the quark-Hadron transition temperature T_c. The momenta distributions are convoluted with the Peterson fragmentation functions of the heavy quark indicated in Eq. 5 in order to get the momentum distribution of D and B mesons.

$$f(z) \propto \frac{1}{[z[1 - \frac{1}{z} - \frac{\epsilon_c}{1-z}]^2]} \tag{5}$$

where $\epsilon_c = 0.04$ for charm quarks and $\epsilon_c = 0.005$ for bottom quark. The ratio between the final distribution (f_f) and the initial distributions (f_i) of the D and B mesons is the nuclear modification factor $R_{AA} = f_i/f_i$ which is shown in figure 2 as a function of p_T for RHIC ($200AGeV$) while in figure 3 the elliptic flow ($v_2 = \langle((p_x^2 - p_y^2)/(p_x^2 + p_y^2))\rangle$) at the same energy as a function of p_T is depicted.

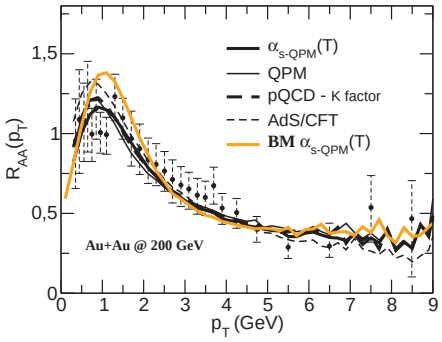

Figure 2. Comparison of the nuclear suppression factor as a function of p_T, obtained with the FP equation at RHIC for the four different T-dependences of the drag coefficient, with the experimental data. The orange line represents the result we obtain using the full Boltzmann equation for the $\alpha_{QPM}(T), m_q = m_g = 0$ case.

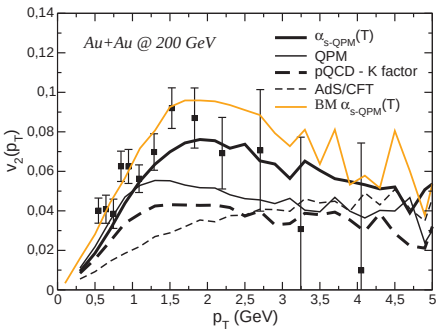

Figure 3. Comparison of the elliptic flow as a function of p_T, obtained with the FP equation at RHIC for the four different T-dependences of the drag coefficient, with the experimental data. The orange line represents the result we obtain using the full Boltzmann equation for the $\alpha_{QPM}(T), m_q = m_g = 0$ case.

In the figures 4 and 5 the R_{AA} and v_2 for LHC ($2.76ATeV$) are shown. As we already mentioned, we set to reproduce the same R_{AA} in all the cases by rescaling the drag coefficient. We observe that even if the R_{AA} is very similar for all the models the build-up of the v_2 is strongly related to the temperature dependence of the drag coefficient. In particular the larger is the interaction in the region of low temperature the larger is the elliptic flow. The same conclusions has been inferred also in the light flavor sector as shown in Refs. [40, 41, 42].

The reason of such a strong dependence of the elliptic flow on the temperature dependence of the drag coefficient is due to the fact that the elliptic flow is generated in the final stage of the evolution of the fireball when the temperature is lower. This is shown in the figures 6 and 7 where the R_{AA} and v_2 are shown at different times. We observe that the R_{AA} is generated

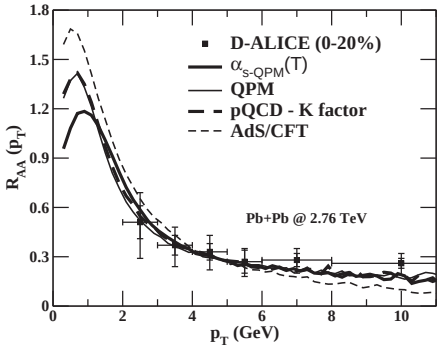

Figure 4. Comparison of the nuclear suppression factor as a function of p_T obtained within FP equation at LHC for the four different T-dependences of the drag coefficient with the experimental data.

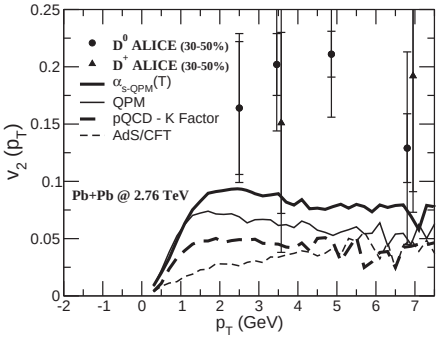

Figure 5. Comparison of the elliptic flow as a function of p_T obtained within FP equation at LHC for the four different T-dependences of the drag coefficient with the experimental data.

in the early stage of the QGP (large T) and is not sensitive to the final stage of the evolution, while the elliptic flow is generated later. This results refer to the pQCD case (*model I*) however the behavior is similar also for the other models.

This study suggests that in order to reduce the difference between the experimental data

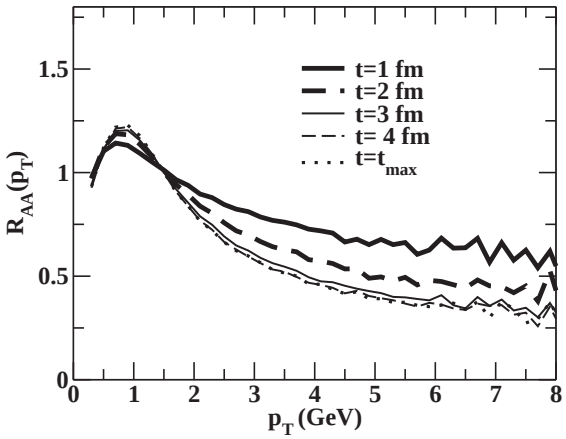

Figure 6. R_{AA} evaluated at different time at RHIC energies ($200AGeV$)

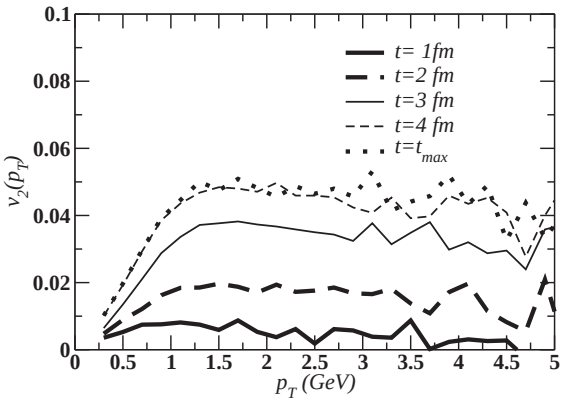

Figure 7. v_2 evaluated at different time at RHIC energies ($200AGeV$)

and the theoretical simulations the drag coefficient of the charm quark cannot increase with a large power of T. The case ($\alpha_{QPM}(T), m_q = m_g = 0$) is the one that can reproduce the experimental data but it is an extreme case used just to have a drag stronlgy decreasing with T. However also the QPM case can be considered quite close to the data considering that two other ingredients can have a substantial impact on the generation of the elliptic flow: the coalescence mechanism that would increase the v_2 for all the cases considered by about 20-25 % [11, 43] and the replacement of the FP equation, based on an expansion of the Boltzmann collision integral up to the second order, with the full collision integral that will be discussed in the next section.

3. Boltzmann approach

The Boltzmann equation for the HQ distribution function is indicated here

$$p^{\mu}\partial_{\mu}f_Q(x,p) = \mathcal{C}[f_Q](x,p) \tag{6}$$

where $\mathcal{C}[f_Q](x,p)$ is the relativistic Boltzmann-like collision integral The collision integral can be written in a simplified form [1, 2] in the following way:

$$\mathcal{C}[f_Q](x,p) = \int d^3k[\omega(p+k,k)f_Q(x,p+k) - \omega(p,k)f_Q(x,p)] \tag{7}$$

where $\omega(p,k)$ expresses the collision rate of heavy quark per unit of momentum phase space. In this work we have not considered radiative processes therefore the heavy quarks interact with the medium by mean of two-body collisions regulated by the scattering matrix of the process $g, q+Q \to g, q+Q$, therefore defining the relative velocity between the two colliding particles as v_{rel} the transition rate can be written as:

$$\omega(p,k) = \int \frac{d^3q}{(2\pi)^3} f_{g,q}(x,p) v_{rel} \frac{d\sigma_{g,q+Q\to g,q+Q}}{d\Omega} \tag{8}$$

The Boltzmann equation is solved numerically dividing the space into a three-dimensional lattice and using the test particle method to sample the distributions functions. The collision integral is solved by means of a stochastic algorithm in which whether a collision happen or not is sampled stochastically comparing the collision probability $P_{22} = v_{rel}\sigma_{g,q+Q\to g,q+Q}\cdot\Delta t/\Delta x$ with a random number extracted between 0 and 1 [44, 45, 30, 46] . We use the Boltzmann equation to describe the propagation of the heavy quark as well as the evolution of the bulk as described in these reference [30, 47].

As emerge from Eq. 7 and from the expression of the collision probability an essential ingredient that has to be specified to study the propagation of the HQ using the BM equation is the cross section that can be calculated from the scattering matrix elements. From the same scattering matrix elements also the drag and diffusion coefficient, that are the keys ingredient of the FP equation, have been calculated. In such way we can make a comparison between the results we get using the BM and those we get using the FP approach having the same interaction.

The comparison between LV and BM approach has been thoroughly studied in these references [25, 26] where it is shown that for bottom quarks the FP is a very good approximation whereas for charm quark FP deviates significantly from the BM and such a deviation significantly depends on the the values of the Debye screening mass. We considered in references [25, 26] three values of m_D: 0.4 GeV, 0.83 GeV and 1.6 GeV. We have shown that the larger is m_D the larger is the difference between the FP approach and the Boltzmann approach. Here we have not considered a fixed value of the Debye screening mass but a value which depends on the temperature according to $m_D = gt$ where g have been evaluated through equation 4. The masses of light quark and gluons have been set equal to zero as it has been done using the Fokker-Planck approach with model *IV* described in section 2. In figures 2 and 3 the comparison for the RAA and v_2 at RHIC between the BM (orange thick line) and the FP (black thick line) are shown. We found that for the same R_{AA} we get a large v_2 using the BM with respect to the R_{AA} we get with the FP.

To summarize our results regarding the different values of elliptic flow that can be obtained using the different models of energy loss, we have introduced in Fig. 8 a new plot in which R_{AA} vs v_2 at a given momentum ($p_T = 1.3$ GeV) is depicted. This plot clearly shows how the building up of the v_2 can differ up to a factor 3 for the same R_{AA} depending on the temperature dependence of the energy loss and on the approach, BM or FP, used to describe the HQ propagation.

With the Boltzmann approach we get a value of the elliptic flow even larger with respect to the experimental data, however as already discussed in section 2, this case represent an extreme

and not realistic case. Moreover to compare with experimental data also the coalescence hadronization mechanism has to be considered. However our results show a non-negligible impact of the approximation in the collision integral involved in the Fokker Plack equation on the relation between R_{AA} and v_2.

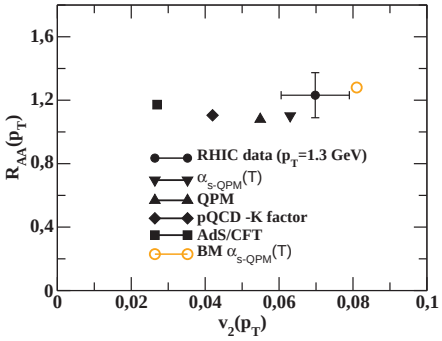

Figure 8. R_{AA} vs v_2 obtained with the FP for the four different T-dependences of the drag coefficient with the experimental data at RHIC energy at $p_T = 1.3GeV$. The open circle indicates the results obtained using the BM approach and the $\alpha_{QPM}(T), m_q = m_g = 0$ case

4. $c\bar{c}$ azimuthal correlations

To further investigate the differences between the FP and the BM approach we have also studied the $c\bar{c}$ correlations at both RHIC and LHC energies. We initialize the $c\bar{c}$ pairs initially in coordinate space accordingly to the binary collisions while in momenta space we have distributed them according to [33]. At the freeze out temperature we evaluate the azimuthal angles $\Delta\phi$ between c and $\bar{c}$ which we have initially distribute in the same point in coordinate space with $p_{T,c} = p_{T,\bar{c}}$, according to the LO initial production. We have performed the simulations in such way to have the same R_{AA} with the FP and the BM approach. We have carried out these simulations using $m_D = 1.6$ corresponding to a quite isotropic cross section which implies the maximum difference between the two approaches.

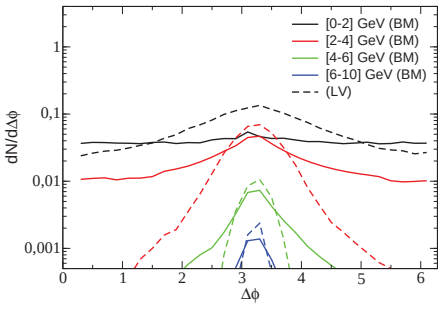

Figure 9. Comparison between $c\bar{c}$ azimuthal correlation at RHIC obtained using the BM (continue lines) and the FP (dashed lines) for different momentum range from $[0, 2]GeV$ (upper part of the figure) to $[6, 10]GeV$ (lower part)

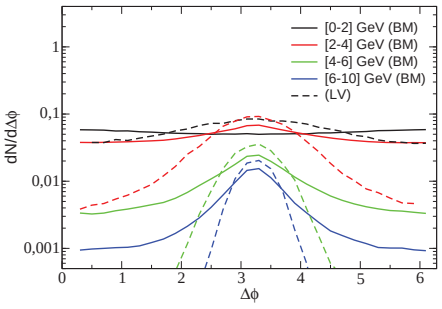

Figure 10. Comparison between $c\bar{c}$ azimuthal correlation at LHC obtained using the BM (continue lines) and the FP (dashed lines) for different momentum range from $[0, 2]GeV$ (upper part of the figure) to $[6, 10]GeV$ (lower part)

The final angular distribution are shown in Fig. 9, for RHIC and in Fig.10 for (LHC) considering four different p_T classes. The pairs are included in a class if both the charm and the anti charm are in the range of rapidity between -1 and 1 and if the momentum of the trigger particle (the one with larger transverse momentum) belongs to a given class. We notice that in all classes of momenta the initial correlations are broadened and the broadening is stronger using the Boltzmann approach. If one look at the lowest momentum class the initial correlation are almost completely washed out in the Boltzmann approach while in Fokker-Plank approach a residual correlation peak is still present. We observe substantial differences in the yield between the BM and the FP.
The reason for such a strong difference for the azimuthal correlations between BM and LV is due to larger spreading of momentum distribution in case of Boltzmann equation in comparison with the Langevin dynamics discussed in Refs [25, 26]. In practice the evolution of a single charm does not appear to be a simply shift in momentum with a Gaussian fluctuations around it. Moreover at LHC we observe in the BM approach an enhancement of the azimuthal correlation in the region of $\Delta\phi = 0$ that is due to the radial flow which push the $c\bar{c}$ in the same direction toward smaller opening angles as pointed out in this Refs [48, 49].

5. Conclusions

We have found that the temperature dependence of the interaction (drag coefficient) is an essential ingredient for the simultaneous reproduction of the nuclear suppression factor, R_{AA}, and elliptic flow, v_2 which is a current challenge almost for all the existing model. We find that typical T-dependence of the drag coefficients can lead to difference in v_2 by 2-3 times even if leading to the same R_{AA}. Our study suggests that the correct temperature dependence of the drag coefficient may not be larger power of T (as in pQCD or AdS/CFT) rather a lower power of T or may be constant in T.
Moreover we have studied the difference in the building up of the elliptic flow between FP and Boltzmann for a fixed R_{AA} and we observe that BM generates a larger elliptic flow [25, 26] than the FP. Finally we have also studied the $c\bar{c}$ correlations at both RHIC and LHC energies to further investigate the impact of the approximation involved in the FP equation. We have found a quite difference in the broadening of the initial correlations between the two approaches. We conclude that the more one look at differential observables (from R_{AA} to v_2 to $c\bar{c}$ azimuthal correlation) the larger is the difference in between FP and BM.

Acknowledgements

We acknowledge the support by the ERC StG under the QGPDyn Grant n. 259684

References

[1] Svetitsky B 1988 *Phys. Rev.* D **37**, 2484
[2] R.Rapp and H van Hees, R. C. Hwa, X. N. Wang (Ed.) Quark Gluon Plasma 4, 2010, *World Scientific*, **111**
[3] A. Adare *et al.* (PHENIX Collaboration), Phys. Rev. Lett. **98**, 172301 (2007).
[4] B. I. Abeleb (STAR Collaboration), Phys. Rev. Lett. **98**, 192301 (2007).
[5] A. Adare*et al.* (PHENIX Collaboration) A. Adare et al. (PHENIX Collaboration), Phys. Rev. C **84** , 044905 (2011)
[6] B. Abelev *et al.*,(ALICE Collaboration) JHEP **1209** (2012) 112
[7] B. Abelev *et al.*,(ALICE Collaboration) Phys. Rev.Lett. **111**,(2013) 102301.
[8] Mustafa M G, Pal D and Srivastava D K 1998 *Phys. Rev.* C **57**, 889
[9] Moore G D, Teaney D 2005 *Phys. Rev.* C **71** 064904
[10] Hees H van, Greco V and Rapp R 2006 *Phys. Rev.* C **73**, 034913
[11] Hees H van, Mannearelli M, Greco V and Rapp R 2008 *Phys. Rev. Lett.* **100** 192301
[12] Akamatsu Y, Hatsuda T, Hirano T 2009 *Phys. Rev.* C **79** 054907
[13] Das S K, Alam J, Mohanty 2009 *Phys. Rev.* C **80** 054916; 2010 *Phys. Rev.* C **82** 014908; Majumdar S, Bhattacharyya T, Alam J, Das S K 2012 *Phys. Rev.* C **84** 044901

[14] Alberico W M *et al.* 2011 *Eur. Phys. J.* C **71** 1666; Alberico W M *et al.* 2013 *Eur. Phys. J.* C **73** 2481
[15] S. Cao, G. Y. Qin and S. A. Bass, Phys. Rev. C **88** (2013) 4, 044907
[16] Lang T, Hees H, Steinheimer J and Bleicher M, arXiv:1208.1643 [hep-ph]
[17] M. He, R. J. Fries and R. Rapp, Phys. Rev. Lett. **110**, 112301 (2013)
[18] F. Riek and R. Rapp, Phys. Rev. C **82**, 035201 (2010)
[19] S. K. Das and A. Davody, Phys. Rev. C **89**, 054912 (2014)
[20] H-J Xu, X. Dong, L-J Ruan, Q. Wang, Z Xu, and Y Zhang, Phys.Rev. C **89** (2014) 024905
[21] S. K. Das, F. Scardina, S. Plumari and V. Greco, arXiv:1502.03757 [nucl-th].
[22] Gossiaux P B, Aichelin J 2008 *Phys. Rev.* C **78** 014904
[23] Uphoff J, Fochler O, Xu Z and Greiner C 2011 *Phys. Rev.* C **84** 024908
[24] J. Uphoff, O. Fochler, Z. Xu and C. Greiner, Phys. Lett. B **717** (2012) 430
[25] S. K. Das, F. Scardina, S. Plumari and V. Greco,Phys. Rev. C **90** 044901 (2014)
[26] F. Scardina,S. K. Das, S. Plumari and V. Greco, J.Phys.Conf.Ser. **535** (2014) 012019
[27] Younus M, Coleman-Smith C E,Bass S A and Srivastava D K, Phys.Rev. C **91** (2015) 2, 024912
[28] T. Song, H. Berrehrah, D. Cabrera, J. M. Torres-Rincon, L. Tolos, W. Cassing and E. Bratkovskaya, arXiv:1503.03039 [nucl-th].
[29] B. Zhang, L. -W. Chen and C. -M. Ko, Phys. Rev. C **72** (2005) 024906
[30] G. Ferini, M. Colonna, Di Toro M. and Greco V, 2009 *Phys. Lett.* **B670**,325; V. Greco ,M. Colonna , Di Toro M and Ferini G, 2009 *Progr. Part. Nucl. Phys.* **62**, 562
[31] S. Plumari,A. Puglisi, F. Scardina and V. Greco, Phys. Rev. C **86** (2012) 054902
[32] V. Greco, C. M. Ko and P. Levai, Phys. Rev. Lett. **90** (2003) 202302; V. Greco, C. M. Ko and P. Levai, Phys. Rev. C **68** (2003) 034904
[33] M. Cacciari, P. Nason and R. Vogt, Phys. Rev. Lett. **95** (2005) 122001; M. Cacciari, S. Frixione, N. Houdeau, M. L. Mangano, P. Nason and G. Ridolfi, JHEP **1210** (2012) 137
[34] B. L. Combridge, Nucl. Phys. B **151**, 429 (1979)
[35] O. Kaczmarek and F. Zantow, Phys. Rev. D, **71**, 114510(2005)
[36] J. M. Maldacena, Adv. Theor. Math. Phys. **2**, 231 (1998)
[37] S. Plumari, W. M. Alberico, V. Greco and C. Ratti, Phys. Rev. D, **84**, 094004 (2011)
[38] S. K. Das, V. Chandra, J. Alam, J. Phys. G **41** 015102 (2014)
[39] H. Berrehrah, E. Bratkovskaya, W. Cassing, P.B. Gossiaux, J. Aichelin, and M. Bleicher, Phys.Rev. C **89**, 054901 (2014)
[40] J. Liao and E. Shuryak, Phys. Rev. Lett. **102** (2009) 202302
[41] F. Scardina, M. Di Toro and V. Greco, Phys. Rev. C **82** (2010) 054901.
[42] X. Zhang and J. Liao, Phys. Rev. C **89**, no. 1, 014907 (2014); J. Xu, J. Liao and M. Gyulassy, arXiv:1411.3673
[43] R. J. Fries, V. Greco, P. Sorensen, Ann. Rev. Nucl. Part. Sci. **58**, 177 (2008)
[44] A. Lang *et al.*, Jour. of Comp. Phys. **106**, 391 (1993)
[45] Xu Z, Greiner C 2005 *Phys. Rev.* C **71**, 064901
[46] F. Scardina, D. Perricone, S. Plumari, M. Ruggieri and V. Greco Phys. Rev. C **90** (2014) 054904
[47] M. Ruggieri, F. Scardina, S. Plumari and V. Greco, Phys. Rev. C **89** (2014) 054914
[48] X. Zhu, N. Xu, and P. Zhuang Phys. Rev. Lett. **100** 152301 (2008)
[49] M.Nahrgang, J. Aichelin, P.B. Gossiaux and Klaus Werner,Phys. Rev. C **90** 024907 (2014)